



Fiber Bragg grating (FBG)-based Hydrophone with side-hole packaging for underwater acoustic sensing

P. Siva Prasad¹ · S. Asokan² · Jaganath Nayak³

Received: 30 June 2021 / Revised: 19 September 2021 / Accepted: 23 September 2021

© Institute of Smart Structures & Systems, Department of Aerospace Engineering, Indian Institute of Science, Bangalore 2021

Abstract

This paper reports design and development of a Fiber Bragg grating (FBG)-based hydrophone with side-hole packaging, for underwater acoustic sensing. The sensing mechanism relies on the variation of birefringence in FBG region under the influence of acoustic pressure. Embedding FBG inside the side-hole package maximizes the pressure on the FBG portion compared with bare FBG. Simulation studies are carried out to optimize the conditions suitable for the packaging and are supported by experimental studies. With the sensor package, a pressure sensitivity of 3200 pm/MPa is achieved which is in good agreement with the simulation results.

Keywords Fiber Bragg grating · Acoustic sensing · Hydrophone · Pressure sensing

Introduction

Listening to underwater sounds is an intense area of research as the acoustic data render a deep insight about enemy intrusions, geophysical structures in the oceans, ocean source localizations, animal vocalizations, etc. (Gannot et al. 2017; Vincent et al. 2018; Mellinger et al. 2016; Gemba et al. 2019; Niu et al. 2017; Gerstoft and Gingras 1996; Deledalle 2019). Existing acoustic transducers such as piezoceramics mainly rely on the conversion of mechanical signals into electrical signals which demand substantial amount of electronics for signal processing and communication of data. These electronics instruments are prone to electromagnetic interferences, spark damages thereby causing blurring and losing of signals (Sherman et al. 2013). Hydrophones based on fiber optics can effectively address these problems because of their advantages such as immunity to electromagnetic

interferences, compatibility to harsh environments, and distributed and multiplexing sensing abilities. Besides the adaptability of miniaturization, sensing multiple parameters at a time is additional advantage of fiber optics (Pevac and Donlagic 2019; Kishore et al. 2017; Pabbiseti 2016; Mihailov 2012).

Linear and nonlinear wavelength modulation of Fiber Bragg gratings (FBG) allow sensing applications for a wide variety of fields like telecommunication, environmental, chemical, defense, medical and other industries (Vengal Rao et al. 2014). Existence of periodic modulation of refractive index in the core of FBG causes a particular wavelength of the light passing through the fiber, which is a function of grating period, to reflect back while remaining wavelengths get transmitted. If any perturbation creates a variation in the periodicity of the grating, the peak of the reflected wavelength would shift, providing a path to sense that particular cause of perturbation. When a FBG is subjected to an acoustic pressure field, its peak undergoes a shift because of the strain caused by the acoustic pressure.

So far, various sensing schemes have been proposed for underwater acoustic sensing, based on FBG principle (Xie et al. 1986; Campopiano et al. 2009; Chimielewska, et al. 2003). However, the large value of Young's modulus of glass material of the fiber forbids the elongation of FBG period, which is a limiting factor of the sensitivity at low pressures. Therefore, an implicit sensing method should be

✉ P. Siva Prasad
shivaprasadparvathaneni@gmail.com

¹ Asymmetric Technologies (DYSL-AT), Hyderabad, Telangana State 500043, India

² Department of Instrumentation and Applied Physics, Indian Institute of Science, Bangalore, Karnataka 560012, India

³ Center for High Energy Systems and Sciences (CHESS), Hyderabad, Telangana 500069, India

designed such that even a low pressure could render a strain on the FBG portion of the fiber.

The present paper demonstrates a method of sensing low pressures by encapsulating the FBG in a polymer material with two side-holes provided on either side of the FBG throughout its length. The provision of two side-holes amplifies the pressure distribution on FBG. Initially, simulation works have been done to understand the suitable conditions and dimensions of the side-holes to amplify the pressure distribution on FBG, and later, the experiment is designed based on the simulated conditions.

Operating principle

Owing to the periodic modulation of refractive index in the core region of the fiber Bragg grating, a particular wavelength of the incoming light into the fiber would be reflected back. The wavelength of the reflected light relies on the pitch and length of the FBG which is given by the equation (Kenneth 1997)

$$\lambda_B = 2n_{eff}\Lambda \tag{1}$$

where n_{eff} represents the effective refractive index of the core at FBG region and Λ is the pitch of the grating. When the FBG undergoes an external perturbation, both the pitch and effective refractive index change thereby emanating a change in the reflected wavelength. The shift in the wavelength can be envisaged by the relation

$$\Delta\lambda_B = \lambda_B(1 - \rho_e)\varepsilon \tag{2}$$

Here, ρ_e is the photo-elastic coefficient and ε is the strain acting longitudinally on the grating.

When the FBG is embedded inside the side-hole package, it will experience an anisotropic stress distribution due to pressure or acoustic perturbations. On account of this anisotropic stress distribution, there occurs a birefringence in the fiber because of the variation in photo-elasticity which leads to a Bragg wavelength shift (Shah Alam and M. xxxx). The main aim of this research is to investigate the methods and to set the suitable parameters for the side-hole package to maximize the stress distribution on FBG portion with the aid of simulation studies.

Simulation

COMSOL multi-physics software is used to simulate the suitable virtual conditions in order to maximize the stress distribution on FBG to carry out the experiment. Figure 1(a) depicts a side-hole package made of polymer designed with the COMSOL used in the present case. It is considered that D_h as the diameter of each side-hole and d

as the distance between the side-holes. The FBG is inscribed in a single mode fiber (SMF) specified with a core diameter of 8 μm and cladding diameter 125 μm . The length of the grating considered is 1 mm and pitch of the grating is chosen to be 540 nm. The refractive index profile of the FBG drawn changes according to the equation

$$n(z) = n_0 + \delta n[\cos\left(\frac{2\pi z}{\Lambda}\right) + 1] \tag{3}$$

where Λ is the pitch of the grating, n_0 is the refractive index of the core in unperturbed condition and δn is the amplitude of the refractive index change caused by applied pressure variation. When the FBG experiences an applied pressure, birefringence would be created due to anisotropic distribution of stress which causes a shift in the FBG peak. The anisotropic stress distribution and geometrical deformations that occur along the cross sections of the fiber are simulated by exercising the structure mechanics module in COMSOL multi-physics software. Applied pressure directions are shown in Fig. 1 (b). Using photo-elastic relations refractive index profiles are obtained as

$$n_x = n_0 - B_1S_x - B_2(S_y + S_z) \tag{4a}$$

$$n_y = n_0 - B_1S_y - B_2(S_z + S_x) \tag{4b}$$

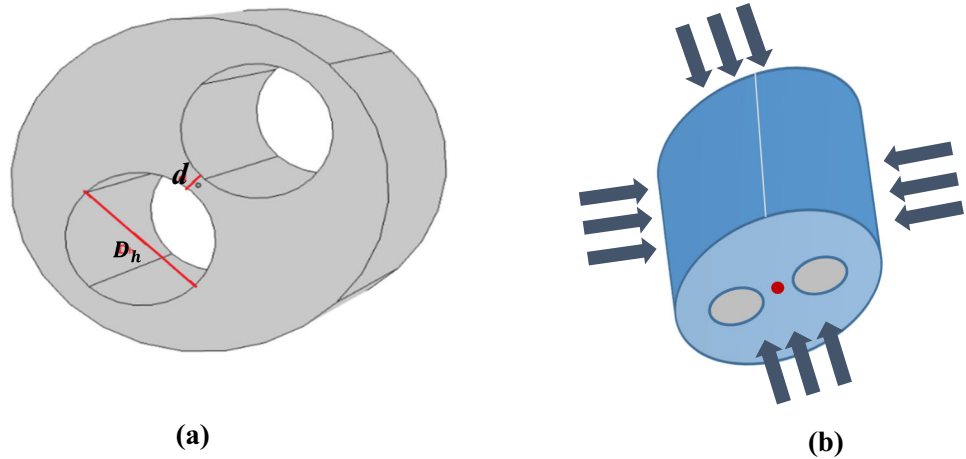
$$n_z = n_0 - B_1S_z - B_2(S_x + S_y) \tag{4c}$$

Here, n_0 is the refractive index of the single mode fiber, B_1 and B_2 are the stress-optic coefficients of the fiber as mentioned in Wu et al. (2011) whose values are given as 6.5e-13m²/N and 4.2e-12m²/N, respectively. S_x, S_y and S_z are the principal stress components along x, y and z axes. By utilizing the above-mentioned refractive index profiles, the fundamental mode of the fiber LP₀₁, under the influence of the applied pressure, is simulated by employing the 3D model of electromagnetic module of the COMSOL software. The following equation is used to estimate the shift of wavelength due to applied pressure (Wu et al. 2010)

$$\Delta\lambda_B = \lambda'_B - \lambda_B\left(\frac{\Delta n_{eff}}{n_{eff}}\right) + \varepsilon_{z,core} \tag{5}$$

where $\Delta n_{eff} = n'_{eff} - n_{eff}$ is the effective index change occurred to applied pressure and $\varepsilon_{z,core}$ is the principal strain in the core of the fiber along the z direction. On setting the refractive index profile of the fiber in three dimensions, intense scrutiny is conducted on simulations to optimize various dimensions of the two side-hole fiber in order to get maximum stress amplification on application of pressure. Different parameters of the side-hole fiber such as diameter of each hole, distance between the holes, length of the side-hole package, outer radius of the package and material suitable for the package are optimized by the simulation studies.

Fig. 1 a Simulated sensor package with side-holes. **b** Pressure distribution on the package



Side-hole package parameters

Upon using the various modules of COMSOL software, key parameters are identified by randomly varying, checking and verifying the conditions for maximization of the stress distribution due to applied pressure. Von Mises stress distribution graphs are considered to decide the parameters. It is identified that RTV-3145 is the suitable material for the packaging material owing to its lower Young’s modulus value which can promote higher pressure amplification. Various parameters finalized on the basis of simulated results are given in Table 1.

Angle between side-hole radius and center of the package

After designing the sensor with parameters as mentioned in above table, it is observed that the angle made by the radius of the side-hole at the center of the package ($\tan^{-1} (AB/OA)$), as shown in Fig. 2, is a pivotal factor in deciding the sensitivity of the sensor. If this angle is around 45° , high sensitivity could be achieved. Upon further increasing the radius of the side-hole such that the angle is more than 45° , then the sensitivity found to show a decreasing trend. However, because of the practical limitations, the angle 45° could not be achieved. The maximum angle that we could

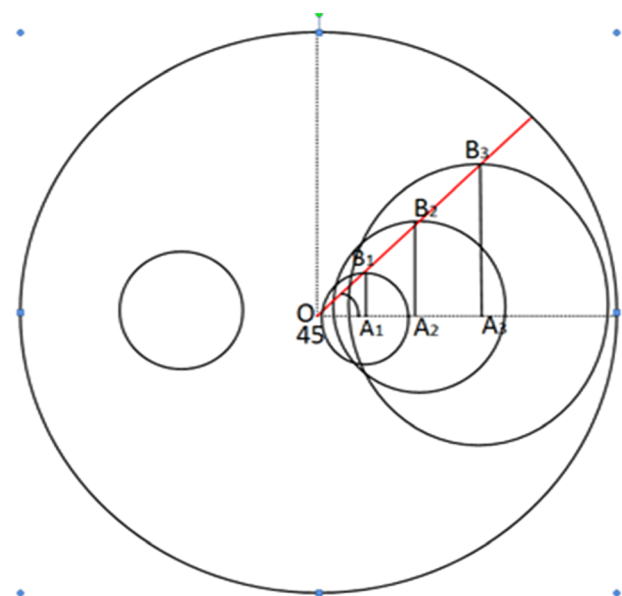


Fig. 2 Angle between the side-hole radius and line joining with center of the package

set between **AB** and **OA** is 43.25° . Hence, the sensor heads are fabricated satisfying this vital specification (Table 2).

Table 1 Simulated parameters of the suitable for the side-hole packaged FBG sensor

Parameters	Value
Radius of the package	17.5(mm)
Length of the package	30(mm)
Package material	RTV3145
Hole size	8.25(mm)
Distance between the holes	500(μ m)

Table 2 Effect of angle on sensitivity of the sensor

Angle $\theta = (\tan^{-1} (\frac{AB}{OA}))$	Sensitivity (pm/MPa)
40.59	912
41.63	1815
42.2	2312
42.7	2625
43.01	2895
43.25	3200

Experiment

Sensor fabrication

A cylindrical hollow Teflon mold, whose dimensions are set according to the simulations, is taken. It contains top cap and bottom cap with a center hole, to pass FBG through it, and two side-holes. The radius and the distance between the side-holes are taken according to the simulation calculations. The fiber is inserted into the mold from center hole of the top cap into the center hole of the bottom cap such that FBG portion is in between the two caps. Later, two solid rods, whose outer radius matches with the radius of the side-holes, are inserted from top cap to bottom cap. Now, a polymer RTV-3145 is poured into the mold and top cap is fixed and the mold with the polymer is left for curing process. The polymer takes about 21 days to get solidified. All the Teflon caps and rod are removed carefully without damaging the sensor.

Experimental setup

Figure 3 depicts the schematic representation of the experimental setup for sensing and quantification of the acoustic pressure. The setup consists of a sensor head in which FBG with 95% reflectivity, having center wavelength at 1535 nm and grating length of 1 cm drawn in a single mode fiber (Corning SMF28), is inscribed in a side-hole polymer package fabricated as described in above section, broadband light source, fiber circulator, fiber optic wavelength interrogator (Smart Scan Interrogator). Polymer package setups for FBG inscription are shown in Fig. 4.

The sensor head with two side-hole package is kept in pressure chamber fitted with a pressure gauge. The pressure applied on the sensor head can be calibrated using the pressure gauge. The one end of the sensor head is firmly attached to a rigid support such that the sensor would not be disturbed during the experiment, whereas the other end is connected to second port of a fiber circulator. A circulator is fiber device having three ports that is used to

transmit light energy to FBG from light source, and also to convey the reflected light from FBG to interrogator/optical spectrum analyzer. A custom-made broadband light source is used to enlighten the sensor head using circulator through port 1. The reflected FBG spectrum is monitored using a fiber optic wavelength interrogator which is having a resolution of 3 pm.

Results and discussion

Characterization of the Sensor toward Pressure sensitivity

Using this experimental setup, the sensor's performance is characterized. Initially, the experiment is conducted with the sensor package having an angle between the radius of the side-holes and the line joining the center of the package as 43.25° . The sensor is fixed firmly in the pressure chamber and pressure is varied from 1 to 10 MPa in steps of 1 MPa. The wavelength shift of FBG is monitored through the interrogator, whereas pressure levels are monitored in the pressure gauge attached to the chamber. The sensor is exposed to each pressure variation for two minutes, and then, the next level of pressure is applied. A bare FBG of similar specifications as the encapsulated FBG is also exposed to pressure under identical condition in order to compare the sensitivity of the polymer-encapsulated FBG with bare FBG. Figure 5 delineates the wavelength of shift of the polymer-encapsulated FBG sensor and bare FBG on the application of pressure on a time scale. It can be observed that as the applied pressure increases, encapsulated sensor demonstrates a tremendous peak shift, whereas bare FBG exhibits a very minor increase which is in the order of picometers (pm) only. This study clearly justifies the sensors potentiality to sense the pressure. An average wavelength shift of 3200 pm/MPa is interposed due to the applied pressure on the encapsulated sensor, whereas bare FBG suffers a maximum of 8 pm/MPa.

Fig. 3 Experimental setup

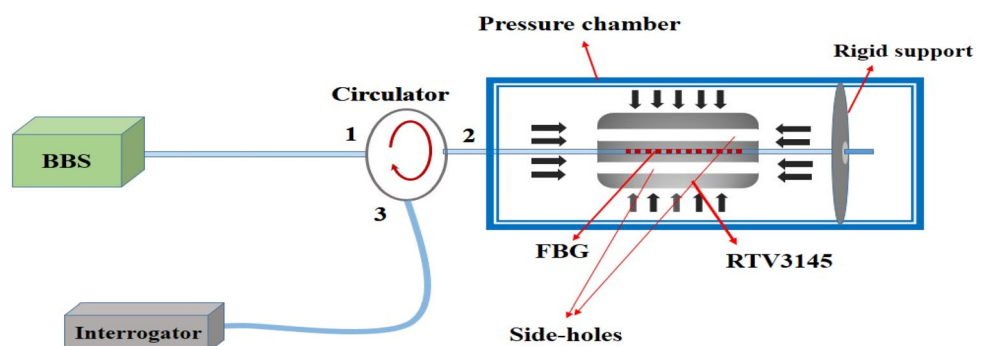
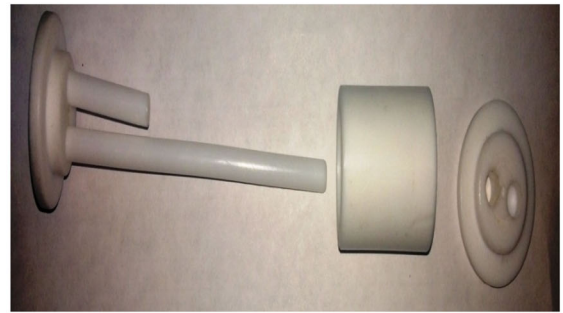


Fig. 4 Polymer package setup for FBG inscription



i) Front view: side hole RTV3145 packaged fibre



ii) Mold: a) Bottom cap with 2 cylinders for side hole
b) Mold structure
c) Top cap with thru-hole



iii) Side view : hole RTV3145 packaged fibre

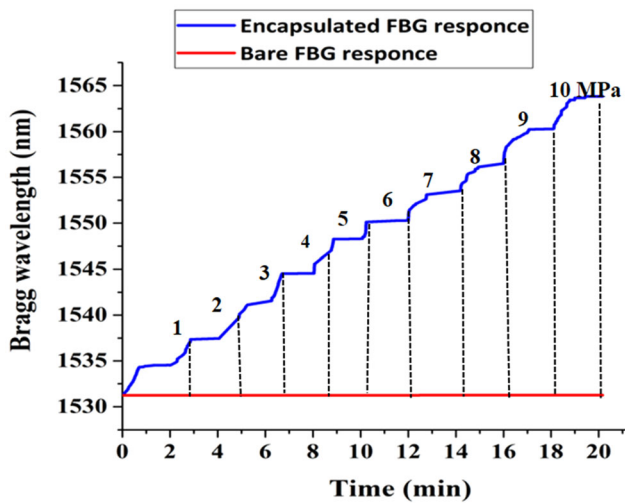


Fig. 5 Response of the encapsulated FBG and bare FBG to applied pressure. (The numbers are in MPa)

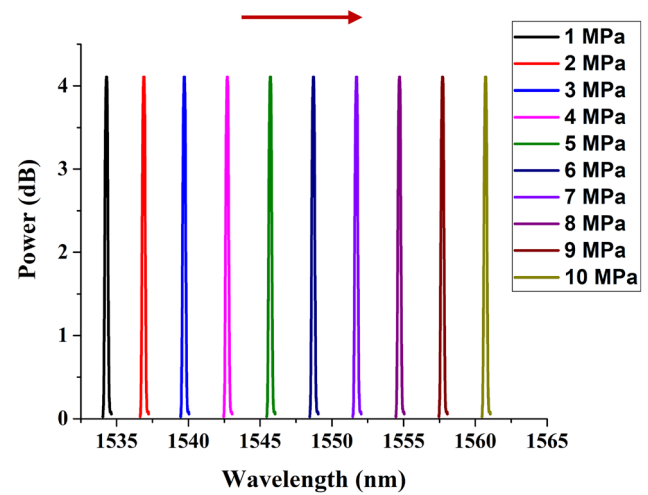


Fig. 6 FBG peak shift of encapsulated sensor corresponding to applied pressure

Thus, the encapsulated sensor package enhances the sensitivity about 1066 times, in comparison with the bare FBG. It is envisaged that the measurement of pressure even in kPa range is also possible by suitable adjustment of the packaging dimensions. The peak-to-peak variation in FBG is shown in Fig. 6 which is an indication of sensors

response toward applied pressure. Further, it can be seen from Fig. 7 that there is a good consistency between experimental and simulated results which proclaims that the side-hole package is the most suitable for pressure sensing.

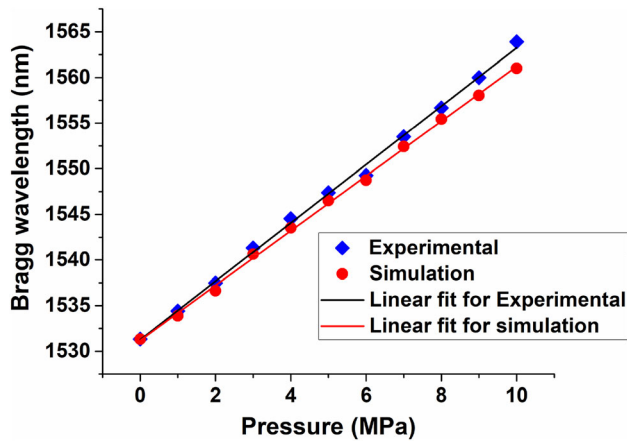


Fig. 7 Comparative study between simulation and experimental results

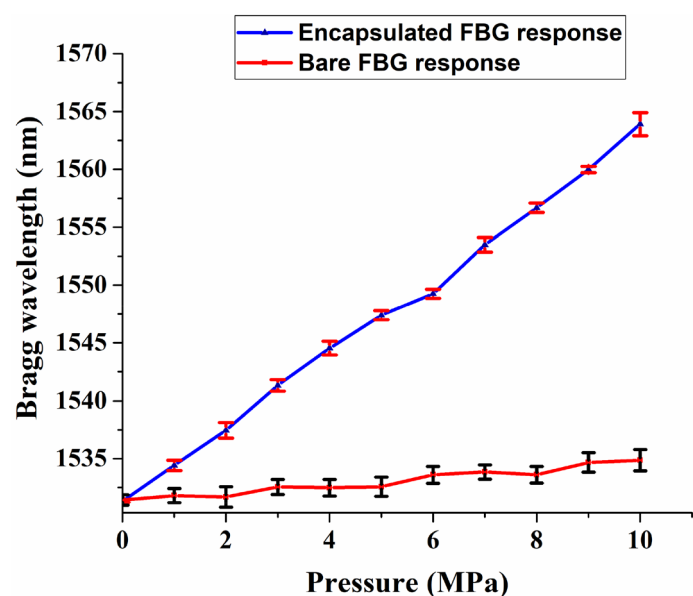
Repeatability

To understand the repeatability of the sensor, the same experiment is repeated for three times. The repeatable nature of the sensor is shown in Fig. 8. In each trail, it is evident that the sensor exhibits identical response with a standard deviation of ± 0.004 nm. The good linearity substantiates the sensor's ability to measure and quantify the ambient pressure, whereas repeatable sensing behavior confirms the adroitness of the sensor for multiple usage. It can also be observed that the deviations are more in bare FBG response though the wavelength shift is very less.

Stability of the sensor

To check whether the sensors response is stable for an applied pressure, the stability studies are carried out. The

Fig. 8 Repeatability of the sensor



sensor is exposed to pressure at a particular value and left for three minutes. As shown in Fig. 9, the sensor displays a stable response throughout the time. The stability study is conducted at pressures of 1 MPa, 2 MPa and 3 MPa.

Sensitivity versus $\theta = (\tan^{-1}(\frac{AB}{OA}))$

As discussed above, simulation studies reveal that the maximum sensitivity can be witnessed if the sensor is designed such that the angle between the radius of the side-holes and line joining the centers of the side-holes with the center of the package that is $\theta = (\tan^{-1}(\frac{AB}{OA}))$, as shown in figure, is 45° . However, practically, it is very difficult to fabricate the sensor package such that the $\theta = (\tan^{-1}(\frac{AB}{OA}))$ is 45° . We have tried various sensor packages with different angles approaching 45° to verify the fact experimentally and the consequent sensitivity studies are also carried out. The following table depicts angle vs sensitivity of various packages.

Conclusions

A Fiber Bragg grating-based hydrophone is proposed and demonstrated to be highly sensitive to even low acoustic pressures. FBG is embedded at the center of a side-hole package fabricated by using a polymer RTV-3145 which lets in a pressure maximization around the FBG portion so that sensor become more sensitive to ambient acoustic variations. Simulation investigations aided to optimize the sensor's specifications and compatible material for sensor package. A pressure sensitivity of 3200 pm/MPa is achieved by the novel side-hole sensor packaging which is

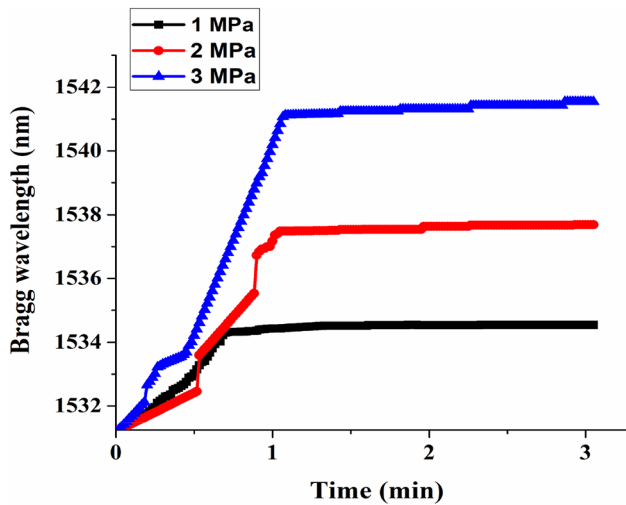


Fig. 9 Stabilization response of the sensor at various pressures

1066 times better than the bare FBG sensitivity. Besides, temperature effect is found to be less on the sensor. It is anticipated that the sensor's sensitivity can be further enhanced by encapsulating etched FBG inside the side-hole packaging.

Declarations

Conflict of interest The authors declared that there is no conflict of interest.

References

- Campopiano S et al (2009) Underwater acoustic sensors based on fiber bragg gratings. *Sensors* 9:4446–4454
- Chmielewska E, Urbańczyk W, Bock WJ (2003) Measurement of pressure and temperature sensitivities of a Bragg grating imprinted in a highly birefringent side-hole fiber. *Appl Opt* 42(31):6284–6291
- Gannot S, Vincent E, Markovich-Golan S, Ozerov A (2017) A consolidated perspective on multimicrophone speech enhancement and source separation. *IEEE Trans Audio Speech Lang Process* 25(4):692–730

- Gemba KL, Nannuru S, Gerstoft P (2019) Robust ocean acoustic localization with sparse Bayesian learning. *IEEE J Sel Top Sign Process* 13(1):49–60
- Gerstoft P, Gingras DF (1996) Parameter estimation using multifrequency range-dependent acoustic data in shallow water. *J Acoust Soc Am* 99(5):2839–2850
- Kenneth OH, Gerald M (1997) “Fiber bragg grating technology fundamentals and overview,” *J Lightwave Technol*, vol.15, No.8
- Kishore PVN, Sai Shankar M, Satyanarayana M (2017) Detection of trace amounts of chromium (VI) using hydrogel coated Fiber Bragg grating. *Sens Actuat B* 243:626–633
- Michael JB, Peter G, James T, Emma O, Marie AR, Sharon G, CharlesAlban D (2019) “Machine learning in acoustics: Theory and applications” *The Journal of the Acoustical Society of America* 146, 3590
- Mellinger DK, Roch MA, Nosal EM, Klinck H (2016) “Signal processing,” in *Listening in the Ocean*, edited by W. W. L. Au and M. O.Lammers (Springer, Berlin, 2016), Chap. 15, pp. 359–409
- Mihailov SJ (2012) Fiber bragg grating sensors for harsh environments. *Sensors* 12:1898–1918
- Niu H, Reeves E, Gerstoft P (2017) Source localization in an ocean waveguide using supervised machine learning. *J Acoust Soc Am* 142(3):1176–1188
- Pabbiseti VNK, Madhuvarasu SS (2016) Hydrogel-coated fiber Bragg grating sensor for pH monitoring. *Opt Eng* 55(6):066112
- Shah MA, Islam MA (2006) “Birefringence Properties of Side-Hole Optical Fibers” Doi: <https://doi.org/10.1109/ICCT.2006.341922> Source: IEEE Xplore 2006
- Sherman DJ, Houser C, Baas ACW (2013) “Electronic measurement techniques for field experiments in process of Geomorphology”, *Treatise on. Geomorphology* 14:195–221
- Simon P, Denis D (2019) Measurement fiber-optic sensors a review. *Opt Eng* 58(7):072009
- Vengal Rao P, Srimannarayana K, Sai Shankar M, Kishore P (2014) Polymer packaged fiber grating pressure sensor with enhanced sensitivity. *Int J Optoelectron Eng* 4(1):1–5
- Vincent E, Virtanen T, Gannot S (2018) *Audio source separation and speech enhancement*. Wiley, New York
- Wu C, Guan B-O, Wang Z, Feng X (2010) Characterization of pressure response of Bragg gratings in grapefruit micro structured fibers. *J Light Wave Technol* 28(9):1392–1397
- Wu C, Li J, Feng X, Guan B-O, Tam H-Y (2011) Side-hole photonic crystal fiber with ultrahigh polarimetric pressure sensitivity. *J Lightwave Technol* 29(7):943–948
- Xie HM, Dabkiewicz Ph, Ulrich R, Okamoto K (1986) Side-hole fiber for fiber-optic pressure sensing. *Opt Lett* 11(5):333–335

Publisher's Note Springer Nature remains neutral with regard to jurisdictional claims in published maps and institutional affiliations.